Advanced Synthesis & Catalysis

DOI: 10.1002/adsc.201400730

The Synthesis of Highly Active Iridium(I) Complexes and their Application in Catalytic Hydrogen Isotope Exchange

Jack A. Brown,[a] Alison R. Cochrane,[a] Stephanie Irvine,[a] William J. Kerr,[a,*] Bhaskar Mondal,[a] John A. Parkinson,[a] Laura C. Paterson,[a] Marc Reid,[a] Tell Tuttle,[a] Shalini Andersson,[b] and Göran N. Nilsson[b]

[a] Department of Pure and Applied Chemistry, WestCHEM, University of Strathclyde, 295 Cathedral Street, Glasgow G1 1XL, Scotland, U.K.
Fax: (+44)-141-548-4822; phone: (+44)-141-548-2959; e-mail: w.kerr@strath.ac.uk
[b] Medicinal Chemistry, AstraZeneca, R&D Mölndal, SE-431 83 Mölndal, Sweden

Received: July 25, 2014; Published online: October 2, 2014

Supporting information for this article is available on the WWW under http://dx.doi.org/10.1002/adsc.201400730.

Abstract: A series of robust iridium(I) complexes bearing a sterically encumbered N-heterocyclic carbene ligand, alongside a phosphine ligand, has been synthesised and investigated in hydrogen isotope exchange processes. These complexes have allowed isotope incorporation over a range of substrates with the use of practically convenient deuterium and tritium gas. Moreover, these active catalysts are capable of isotope incorporation to particularly high levels, whilst employing low catalyst loadings and in short reaction times. In addition to this, these new catalyst species have shown flexible levels of chemoselectivity, which can be altered by simple manipulation of preparative approaches. Furthermore, a number of industrially-relevant drug molecules has also been labelled, including the sulfonamide containing drug, Celecoxib. Alongside detailed NMR experiments, initial mechanistic investigations have also been performed, providing insight into both substrate binding energies, and, more importantly, relative energies of key steps in the mechanistic cycle as part of the overall exchange process.

Keywords: catalysis; deuterium; hydrogen isotope exchange; iridium; tritium

Introduction

Despite colossal financial commitment to drug discovery, the pharmaceutical industry is burdened by unsustainable attrition rates associated with new chemical entities. Accordingly, positioning metabolism and pharmacokinetic studies earlier in such discovery programmes is crucial in assessing the overall properties of a drug candidate and as aligned to reducing the present levels of attrition of over 90%.[1] One key methodology applied extensively within this area is isotopic labelling, which allows the biological fate of a potential drug molecule to be carefully monitored.[2] In particular, transition metal-catalysed hydrogen isotope exchange (HIE) offers a simple and direct technique, which potentially allows the regioselective labelling of fully functionalised molecules (Scheme 1), eliminating the need for any additional synthetic processes or prolonged preparative pathways associated with the installation of an isotopic label.

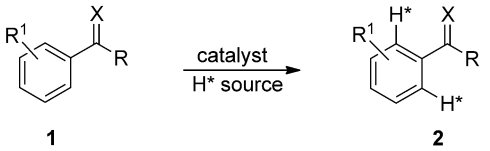

1 2

Scheme 1. Ideal hydrogen isotope exchange process.

Whilst various transition metal species have demonstrated activity within the field of HIE,[3–6] for a number of years $[Ir(COD)(PCy_3)(py)]PF_6$, Crabtree's catalyst,[7] was regarded as the industry standard to facilitate such a process. This iridium-based complex demonstrates appreciable activity in the labelling of a range of substrates, however, it is often found that (super-)stoichiometric quantities of the catalyst and lengthy reaction times are required to deliver the observed levels of isotope incorporation.[8] In addition, tritiation reactions promoted by Crabtree's catalyst frequently produce considerable quantities of radioactive waste, which is a clear drawback with

 © 2014 Wiley-VCH Verlag GmbH & Co. KGaA, Weinheim

regard to both cost and environmental concerns.[2c,9] In view of the issues associated with Crabtree's catalyst, it is evident that alternative metal-based complexes for use in hydrogen isotope exchange would be beneficial to pharmaceutical partners with, in particular, the desired catalysts being capable of labelling an assortment of substrates to high levels of incorporation under mild reaction conditions and with lowered catalyst loadings. Following the work of Nolan[10] and Buriak[11] in the field of olefin hydrogenation, we felt that in order to enhance catalytic activity in HIE processes, relative to Crabtree's catalyst, greater steric demand around the metal centre, coupled with balanced electronic parameters, was required.[12] In this regard, we have reported on the preparation and application of a series of new iridium complexes bearing a bulky N-heterocyclic carbene (NHC), 1,3-bis(2,4,6-trimethylphenyl)imidazol-2-ylidene (IMes), alongside an appreciably encumbered phosphine, and which have appreciable potential as highly active catalysts for HIE with deuterium.[13] Additionally, we have shown that these robust and practically accessible iridium species can be applied within the selective reduction of alkenes (and alkynes)[14] and in the *Z*-selective dimerization of terminal alkynes.[15]

Herein, we report the activity and selectivity spectrum of this class of iridium complex in the area of deuterium and, importantly, tritium labelling, as well as our initial investigations into the overall mechanism of the hydrogen isotope exchange process with these emerging catalyst species.

Results and Discussion

First of all, and importantly in a practical sense, a robust and readily utilisable route to our novel Ir(I) complexes bearing a sterically encumbered NHC in conjunction with a bulky tertiary phosphine ligand was achieved according to a variation of a procedure delineated by Herrmann.[16] The use of sodium ethoxide in the relatively weakly coordinating solvent, benzene, was crucial to allow the *in situ* generation and introduction of the NHC ligand, avoiding the necessity to pre-form and isolate the free carbene species under glove-box conditions. Following this modified synthetic route, five novel Ir(I) complexes were delivered in good yields (Table 1). These bright red catalysts are air- and moisture-stable crystalline solids, and have been characterised by NMR and mass spectral techniques. In addition, the structures of complex **5a–c** have been confirmed by X-ray crystallography.[13a]

Under the standard reaction conditions developed within our laboratory, employing a catalyst loading of 5 mol% in DCM under 1 atmosphere of D_2 gas for 16 h, complexes **5a–e** facilitated high levels of H/D

Table 1. Preparation of iridium complexes.[a]

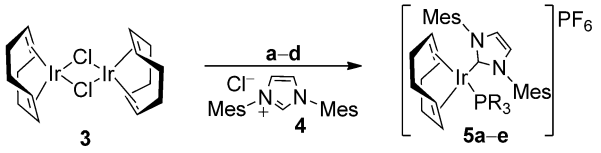

Entry	PR_3	Complex	Yield[b]
1	PPh_3	**5a**	62
2	PBn_3	**5b**	59
3	PMe_2Ph	**5c**	71
4	$PMePh_2$	**5d**	69
5	$P(O\text{-}i\text{-}Pr)_3$	**5e**	75

[a] *Reaction conditions:* (a) NaOEt, PhH, room temperature, 10 min. (b) **4**, PhH, room temperature, 5 h. (c) $AgPF_6$, THF, room temperature, 30 min. (d) PR_3, THF, room temperature, 2 h.
[b] Isolated yields.

exchange across a wide range of substrates (**6a–i**) including ketones, amides, and heterocyclic functionalities (Table 2). In general, compounds **7a–g**, which are labelled *via* a 5-membered metallocyclic intermediate (5-mmi), were delivered with high deuterium incorporations in a regioselective and reproducible manner. Furthermore, the isotopic labelling of weakly coordinating nitrobenzene, **6g**, proceeded without incident and with no reduction of the nitro moiety, as has been detected with previously employed catalysts.[5f,8b] It is important to highlight that the levels of isotope exchange in benzamide, **6c**, were somewhat more variable, ranging from 32% in the presence of complex **5a**, to 90% in reactions catalysed by complex **5d**. Indeed, this substrate is notoriously difficult to label effectively, with 110 mol% of Crabtree's catalyst being previously required to deliver the isotopically-enriched product with only a moderate 65% D incorporation.[8b] The examination of additional substrates revealed the ability of our novel Ir(I) complexes to also facilitate isotope exchange in C–H units positioned five bonds away from the required coordinating functionality i.e., *via* a 6-membered metallocyclic intermediate (6-mmi). This process is believed to be energetically more demanding and, as such, often leads to lower levels of deuteration. In our hands, the simplest substrate of this class, acetanilide, **6h**, was labelled up to an excellent 95% D loading. Furthermore, deuterium incorporation in benzanilide, **6i**, occurred with high degrees of exchange observed in positions labelled *via* both a 5-mmi and a 6-mmi.

To further explore the capabilities of our complexes, a series of rate and activity studies was performed. A loading study revealed that excellent deuterium incorporation is maintained in the presence of catalyst quantities as low as 0.5 mol% (Scheme 2). Furthermore, whereas catalyst **5a** mediated the 97%

 © 2014 Wiley-VCH Verlag GmbH & Co. KGaA, Weinheim

Table 2. HIE studies with complexes **5a**–**e**.[a,b]

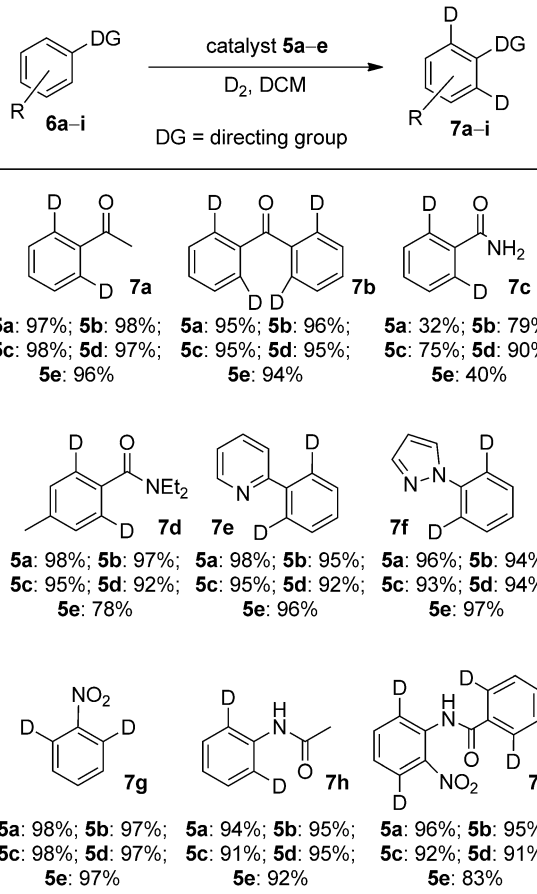

[a] 5 mol% of Ir catalyst employed over 16 h.

[b] Average incorporation into the positions shown over two separate reaction runs; the percentage given refers to the level of D incorporation over the total number of positions shown, for example, 97% for the two possible positions in **7a** indicates 1.94 D incorporation.

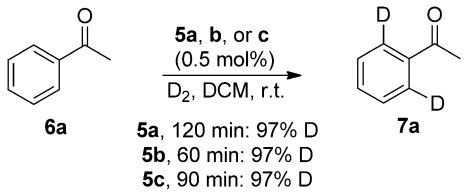

Scheme 2. Catalyst loading and labelling time study.

deuteration of **6a** within 120 min, more electron-rich catalysts, **5b** and **5c**, delivered more rapid labelling (60 and 90 min, respectively). Presumably, the more electron-rich catalysts better facilitate the C–H activation process central to the H/D exchange reaction.[17]

The excellent levels of efficiency displayed by these complexes prompted us to examine their catalytic activity further. As demonstrated in the labelling of **6i** (Table 2), benzanilide substrates offer two potential sites of labelling, through either a 5- or 6-mmi. It was therefore proposed that the emerging catalysts had the potential to exert regioselective deuteration in substrates of this type. Such discrimination of H/D exchange in one position over another would be of particular benefit to pharmaceutical partners, allowing specific drug metabolites to be traced preferentially during *in vivo* distribution studies. In an attempt to establish such selective HIE, the labelling of benzanilide **6j** was studied. As illustrated in Scheme 3, the use of 5 mol% of complex **5c** delivered appreciably high levels of isotope incorporation in both positions *a* and *b*. In contrast, reducing the amount of catalyst present in the reaction system to 0.5 mol% resulted in a significant decline in the degree of labelling observed in position *b*, *via* a 6-mmi, while the elevated level of exchange in position *a*, proceeding *via* the more favourable 5-mmi, was maintained. A similar result was obtained with the benzanilide derivative **6k**, which is capable of labelling through both a 5- and a 6-mmi at three possible sites in the molecule. At a 5 mol% catalyst loading, complex **5c** showed excellent levels of incorporation into positions *a* and *b* (both *via* a 5-mmi), while position *c* (*via* a 6-mmi) showed more moderate D uptake. Pleasingly, when the catalyst loading was reduced to 0.5 mol%, not only did we again observe exclusive labelling *via* the 5-mmi over the 6-mmi, there was also selectivity noted between positions *a* and *b*. The preferential labelling at position *a* suggests more effective iridium metal centre coordination with the more available oxygen lone pairs within the amide carbonyl group over the oxygen atoms of the nitro unit.

Based on these findings, it was envisaged that our overall protocols could be manipulated to achieve selective labelling into a position labelled *via* a 6-mmi (Scheme 4). This was accomplished by employing the heavily labelled compound **7j** (*a*: 96%; *b*; 93%) as substrate with H_2 to allow H exchange at position *a*, leaving the deuterium in place at position *b*. As

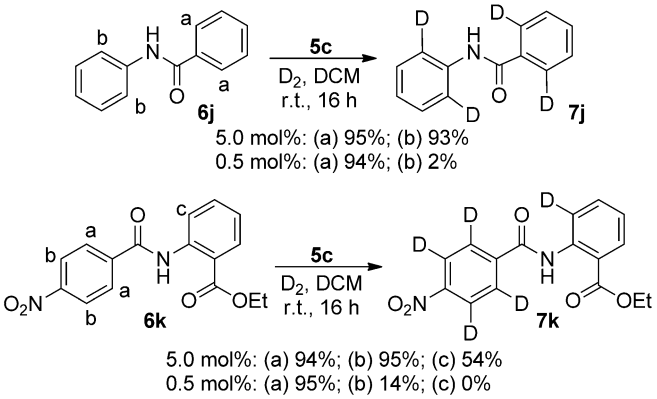

Scheme 3. Labelling selectivity for a 5-mmi over a 6-mmi.

 © 2014 Wiley-VCH Verlag GmbH & Co. KGaA, Weinheim

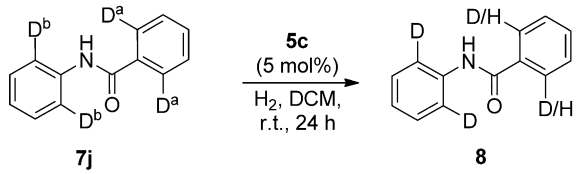

Scheme 4. Selective removal of the D label *via* the 5-mmi.

shown in Scheme 4, employing 5 mol% of complex **5c** under an atmosphere of hydrogen resulted in the selective removal of deuterium *via* the 5-mmi, while the level of D at position *b* remained high. Accordingly, this section of our study has shown that it is now possible to access both classes of selectively labelled compounds, which illustrates a further distinct practical advantage delivered by these novel iridium catalyst systems. To the best of our knowledge, this level of labelling selectivity by this direct approach is unprecedented in the literature.

To further illustrate the capabilities of these catalysts, a number of available drug molecules was applied in hydrogen isotope exchange reactions. The ability to label fully functionalised drug scaffolds is central to the application of HIE catalysis, especially as aligned to the endeavours of pharmaceutical partners. Pleasingly, complexes **5a–c** performed very well with a series of drug substrates at relatively low catalyst loadings and over short reaction times (**7l–o**; Table 3). Of particular note is the high level of D incorporation in the Pfizer COX-2 inhibitor, Celecoxib,

Table 3. HIE studies with marketed drug molecule substrates.

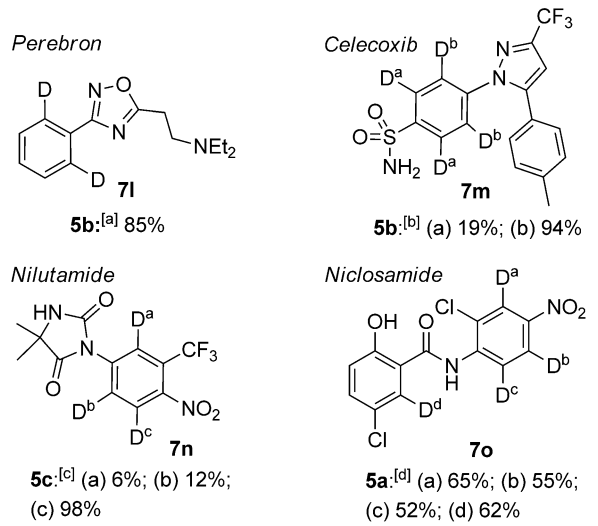

[a] 5 mol% of Ir catalyst employed over 16 h.
[b] 10 mol% of Ir catalyst employed over 1 h.
[c] 2.5 mol% of Ir catalyst employed over 1 h.
[d] 5 mol% of Ir catalyst employed over 1 h.

Table 4. Catalyst turnover.

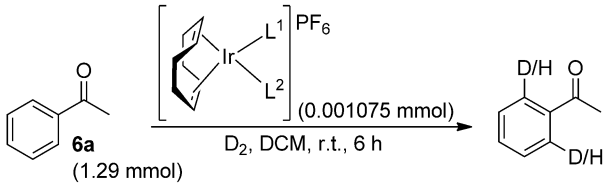

Entry	L^1/L^2 (catalyst)	% D	TON[a]	TOF[b]
1	IMes/PBn_3 (**5b**)	88	1056	176
2	Py/Ph_3P (Crabtree's)	29	348	58

[a] Measured as no. moles of substrate converted/no. moles of catalyst employed.
[b] Measured as no. moles of substrate converted/no. moles of catalyst employed/hours.

7m. In addition to the high level of D uptake obtained in position *b*, the D incorporation at position *a* represents the first example of deuterium labelling adjacent to a primary sulfonamide moiety as facilitated by complexes of this type,[18] albeit at relatively moderate levels. Furthermore, Sanofi–Aventis' antiandrogen Nilutamide, **7n**, provides a further example of preferential labelling *via* a 5-mmi over a 6-mmi.

Following the exploration of substrate scope, we sought to gain further insight regarding the effectiveness of our novel system *via* the analysis of catalyst turnover. As shown in Table 4, the deuteration of acetophenone using catalyst **5b** delivered very good turnover within a 6 h reaction period, using extremely low levels of catalyst. Under the same conditions, Crabtree's catalyst showed a vastly reduced efficiency; presumably due to its lower relative activity and instability over time.[12]

Mechanistic Investigations

Although the mechanism of iridium-catalysed HIE was proposed by Heys in 1996,[5d] there exists only limited evidence to support the perceived sequence of events.[5o] Therefore, we were interested in embarking upon focused mechanistic investigations to increase the general comprehension of such catalysed hydrogen isotope exchange process. Furthermore, by embedding our emerging iridium complex class within this study, we envisaged that any enhanced understanding could provide beneficial foundations to be used in the design of future catalyst systems.

Initially and to this end, an exchange reaction was carried out in an NMR tube, using deuterated dichloromethane, to allow us to monitor two key features in the proposed pathway: the initial removal of the cyclooctadiene (COD) unit from the iridium complex, and the resultant geometry of the major ligands around the metal centre. Since the formation of iridi-

 © 2014 Wiley-VCH Verlag GmbH & Co. KGaA, Weinheim

um hydrides is thought to be central to the removal of the COD ligand, the reverse exchange reaction (Scheme 5) was carried out by employing fully deuterated acetophenone **9** and exchanging with hydrogen gas, in an attempt to observe any potential Ir-hydride species. Complex **5a** was chosen as this is the slowest acting of this series of catalysts, with 10 mol% being employed in order to fully observe intermediate com-

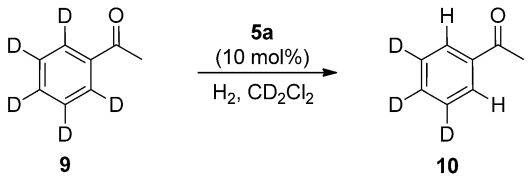

Scheme 5. Reverse exchange reaction monitored in an NMR tube.

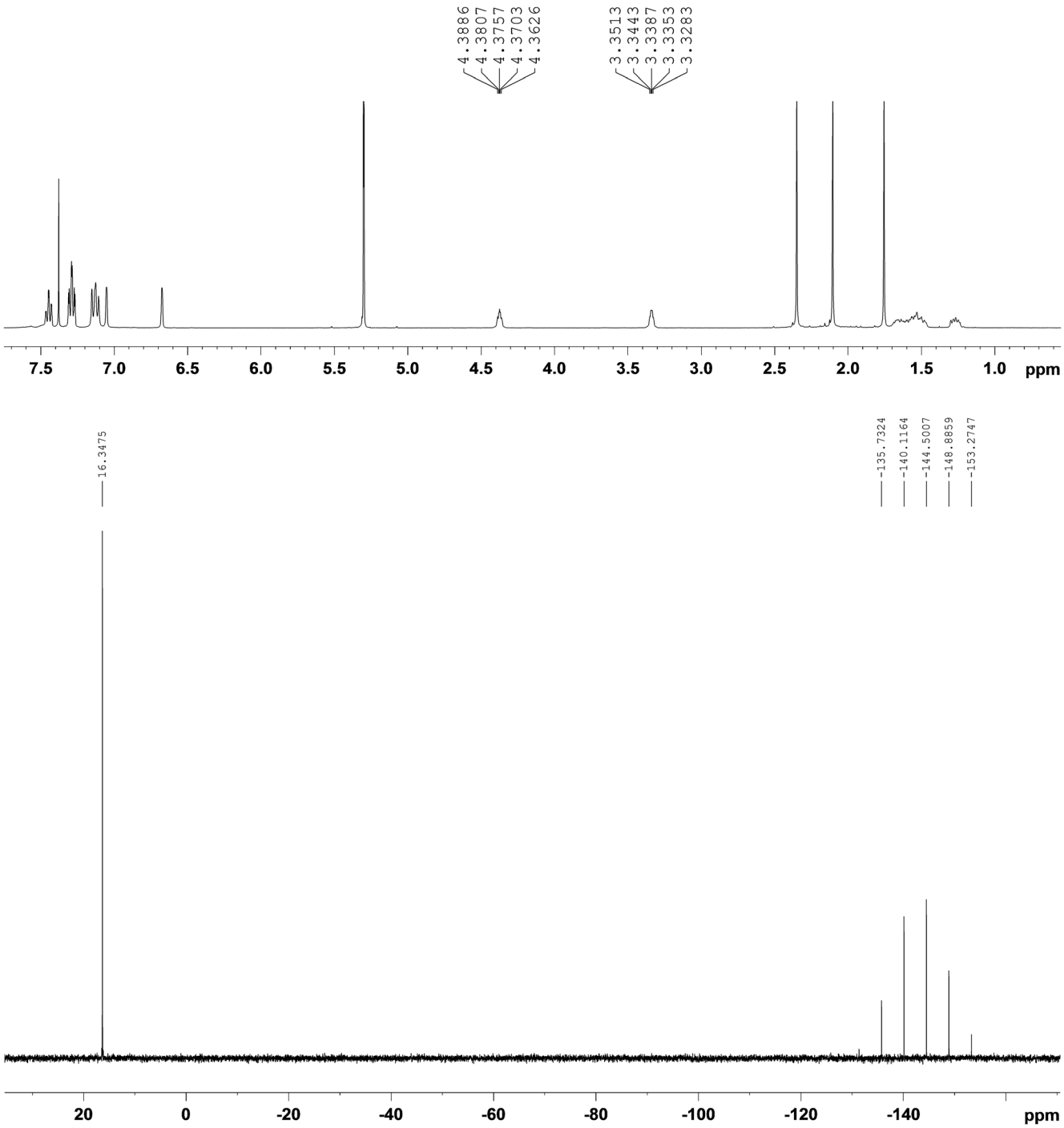

Figure 1. ^{1}H (*top*) and ^{31}P (*bottom*) NMR spectra of complex **5a** in CD_2Cl_2.

 © 2014 Wiley-VCH Verlag GmbH & Co. KGaA, Weinheim

plexes and reaction progression by NMR analysis (see the Supporting Information for full details).

Prior to the monitoring of the reaction, it was necessary to gather data on the parent complex, to allow the detection of any changes that occur as the overall process progresses. Accordingly, ^{1}H and ^{31}P NMR spectra of complex **5a** were obtained in CD_2Cl_2. The most relevant ^{1}H spectrum peaks at the beginning of the reaction were the multiplets at 4.39–4.36 and 3.35–3.33 ppm, as shown in Figure 1. These peaks correspond to the olefinic protons of the COD ligand, and are expected to lose intensity and disappear at the beginning of the reaction as the COD is reduced. With regard to the ^{31}P NMR, the peak present at 16.35 ppm corresponds to the phosphine ligand bound to the metal centre.

Figure 2 shows a 2D $^{31}P/^{13}C$ HMQC experiment of the same parent complex **5a**. This allowed the $^{2}J_{P,C}$ coupling constant between the bound phosphorus atom and the carbon of the carbene ligand to be established. It was envisaged that by carrying out this correlation experiment as the reaction proceeds, the observed magnitude of this $^{2}J_{P,C}$ coupling constant would provide some indication of the geometry of the two major ligands. As presented in Figure 2, a distinct correlation was observed between the bound phosphine at 16.35 ppm and the carbene carbon at 177 ppm. The $^{2}J_{P,C}$ coupling constant was measured at 8.6 Hz, in accord with these two ligands adopting a *cis*-arrangement in the parent complex. In turn, we were confident that the geometry of the ligands in any reaction intermediates could then be deduced by comparing the coupling constants obtained throughout the reaction. Consequently, the reaction (Scheme 5) was performed in an NMR tube using d_5-acetophenone **9** and hydrogen gas, with CD_2Cl_2 as the reaction solvent. Following the initial addition of hydrogen gas, several peaks emerged in the ^{1}H NMR spectrum in the region of −13–0 ppm, indicating the presence of the expected iridium hydrides. The reaction was then further monitored to assess the reduction and removal of the COD ligand, as shown by the disappearance of the multiplet peaks at 4.39–4.36 and 3.35–3.33 ppm; importantly, following this further analysis the peaks corresponding to the iridium hydrides had also disappeared, suggesting that these hydrides play a key role in the removal of the COD ligand. Furthermore, in the absence of the COD ligand, ^{31}P NMR analysis showed that the original phosphine signal (16.35 ppm) had been replaced with a new peak at 20.80 ppm, indicating that the parent complex had been fully converted to an alternative phosphorus-containing iridium species within the reaction manifold.

To further investigate the new COD-free iridium intermediate, a second 2D HMQC $^{13}C/^{31}P$ correlation spectrum was obtained. As illustrated in Figure 3, the carbene carbon signal at 177 ppm had been replaced by a new signal at ~160 ppm. This change in chemical shift was accompanied by a correlation to the phosphine signal at 20.80 ppm, and with an appreciably elevated $^{2}J_{P,C}$ coupling constant of 118 Hz. Indeed, such large $^{2}J_{P,C}$ coupling constants in similar iridium complexes, bearing phosphine and NHC ligands, have some literature precedent. For example, iridium(I) complex **11**, depicted in Figure 4, has been shown to have the triphenylphosphine and bis-benzyl NHC ligands in a relative *trans*-arrangement.[19a] The data for this compound reveal the carbene carbon of the NHC to have a chemical shift of 177.6 ppm and a $^{2}J_{P,C}$ coupling constant of 116 Hz. In an analogous manner, iridium(III) complex **12** has the triisopropylphosphine

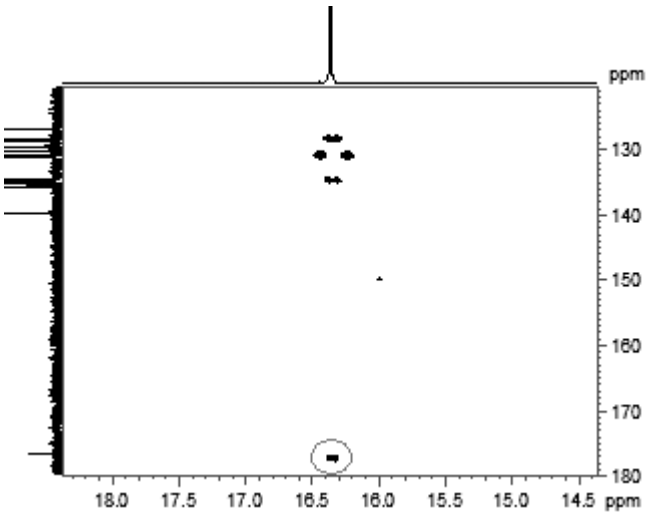

Figure 2. 2D $^{31}P/^{13}C$ HMQC experiment of the parent complex.

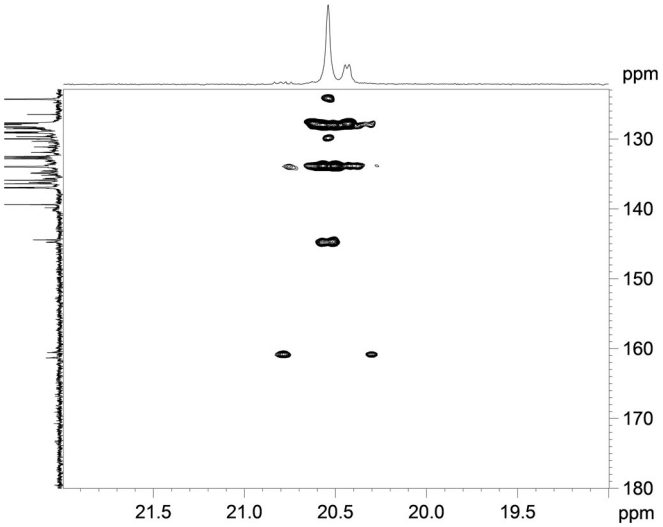

Figure 3. 2D $^{31}P/^{13}C$ HMQC spectrum of intermediate Ir complex.

© 2014 Wiley-VCH Verlag GmbH & Co. KGaA, Weinheim

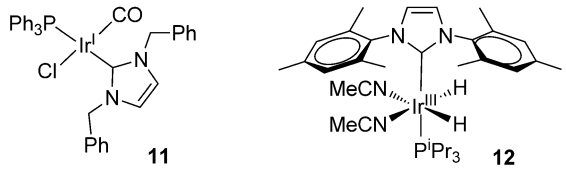

Figure 4. Known Ir complexes with phosphine/NHC ligands in a *trans*-arrangement.

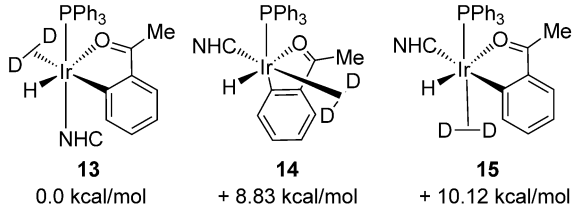

Figure 6. Optimised structures of **13** and its isomers at DFT level.

and IMes ligands in a *trans*-configuration, with a similar $^{2}J_{P,C}$ coupling constant value of 108 Hz.[19b] However, the chemical shift of the carbene carbon in this latter complex is significantly more upfield than that of complex **11**, with a value of 165 ppm. From the evidence obtained regarding the activated catalytic species in our HIE reaction, and from comparison with available literature data,[19] it is proposed that the intermediate within this manifold has the phosphine and NHC ligands in a *trans* geometry; furthermore, the ^{13}C NMR chemical shift of the carbene carbon is consistent with this new catalytic intermediate possessing an iridium(III) oxidation state.

To further support the above experimental evidence that the phosphine and NHC ligands align themselves in a *trans*-configuration, density functional theory (DFT) studies (see the Supporting Information for full details on the level of theory used) were employed to calculate the relative energies of the proposed *cis*- and *trans*-isomers of the intermediate iridium species. Using Heys' mechanism as a guide,[5d] the most sterically hindered species along the catalytic cycle is envisaged to be that formed subsequent to oxidative insertion with the substrate, for example, **13** with acetophenone (Figure 5). Therefore, the energetic ordering of the possible isomers of **13** was investigated to determine the probable active configuration within the HIE manifold.

Potential orientations of the D_2, hydride, and substrate ligands were investigated; however, all alternative configurations converged to one of the three isomers shown in Figure 6. In addition to the *trans*-isomer **13**, two *cis*-isomers were also optimised to local minima on the potential energy surface (**14** and **15**, Figure 6). The relative energies of the three isomers indicate that **14** and **15** are destabilised by 8.83 and 10.12 kcal mol^{-1}, respectively, relative to **13**. These findings support the experimental evidence that the phosphine and NHC adopt a *trans*-orientation within the activated Ir species.

Our DFT calculations were further expanded to focus on the possible reaction pathway by which hydrogen isotope exchange proceeds. These more detailed investigations allowed the construction of the potential energy surface (PES) associated with the proposed catalytic cycle. Using that suggested by Heys as a basis,[5d] a mechanistic pathway employing our Ir(I) complexes in conjunction with acetophenone, **6a**, was determined (Scheme 6). It is proposed that, following exposure to deuterium gas, complex **5a** loses the COD ligand as d_4-cyclooctane. The resulting coordinately unsaturated Ir species is stabilised by coordination of the substrate, for example, **6a**, delivering

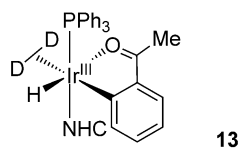

Figure 5. Oxidative addition intermediate in the catalytic cycle.

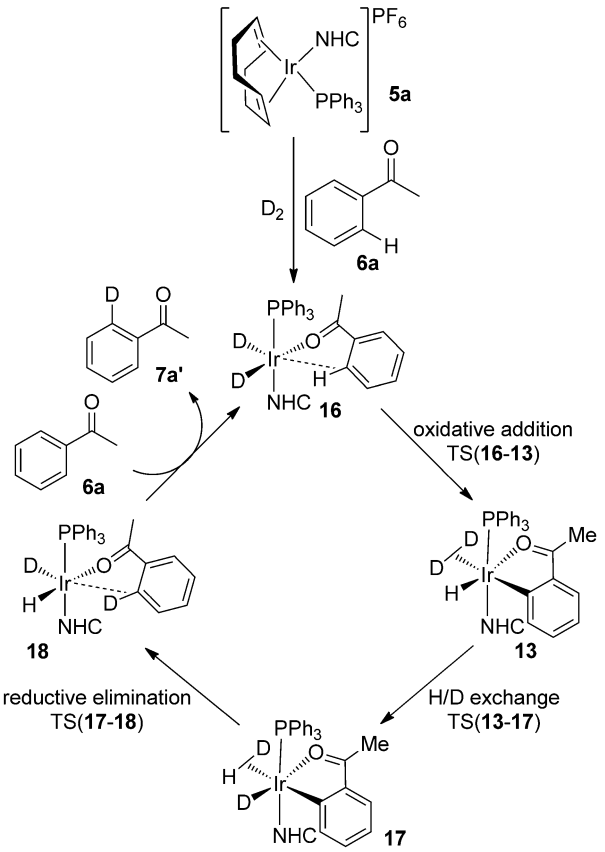

Scheme 6. Proposed HIE catalytic cycle.

 © 2014 Wiley-VCH Verlag GmbH & Co. KGaA, Weinheim

16. Following oxidative addition to give **13**, fluxionality of the dihydrogen hydride (**13**→**17**) allows isotopic hydrogen to orient in the position *cis* to the Ir–C bond, resulting, ultimately, in reductive elimination (**17**→**18**) and isotope incorporation into the *ortho*-position of the substrate aryl ring, **7a′**. In relation to modifications to Heys' original mechanistic scheme, we now believe that the initial activated iridium species is stabilised by association of the substrate forming complex **16** in which the *ortho* aryl C–H is agostically coordinated to the iridium centre. Furthermore and in a more general sense, a series of ^{31}P NMR magnetization transfer experiments, analogous to the work of Grubbs' within the field of ruthenium-catalysed olefin metathesis,[20] indicates that the phosphine ligand does not dissociate from the iridium metal centre throughout the catalytic cycle (see the Supporting Information for experimental details).

All of the intermediates and transition states involved in our proposed catalytic cycle, with the incorporation of deuterium, have been fully optimised. Therefore, the enthalpy changes during the reaction progress have been monitored. Relative enthalpies of the stationary points on the PES and the barriers to oxidative addition, H/D exchange, and reductive elimination have also been calculated for each species shown in Scheme 6. In addition to the use of PPh_3 and in order to probe the possibility of performing computational studies of more minimised cost, PMe_3 was also investigated as the axial phosphine ligand (Table 5). The decreased ligand size in the PMe_3 systems does not alter the mechanism of the reaction, nor does it strongly affect the geometry of the ligands around the equatorial plane, i.e., there is no large rearrangement of the ligands and the changes in bond lengths between the full (PPh_3) systems and the trimmed (PMe_3) version are calculated to be in the region of 0.02 Å (see the Supporting Information for details). Comparing the calculated energetic parameters detected along the reaction path for both PPh_3 and PMe_3 (Table 5), the axial phosphine substituent has a detectable impact on the energy of the oxidative addition step, with a difference of 1.43 kcal mol^{-1} calculated for TS(**16**-**13**) between the species bearing PPh_3 and the smaller PMe_3.

Table 5. Relative energies (ΔE), enthalpies (ΔH), and Gibbs free energies (ΔG) for the catalytic cycle calculated at DFT level (all are in kcal mol^{-1}).

	ΔE[a]		ΔH[b]		ΔG[b]	
Species	PPh_3	PMe_3	PPh_3	PMe_3	PPh_3	PMe_3
16	0.00	0.00	0.00	0.00	0.00	0.00
TS(**16**-**13**)	17.21	18.14	16.70	18.13	18.65	18.35
13	3.33	0.93	3.66	1.20	2.88	0.27
TS(**13**-**17**)	5.86	3.17	5.91	3.66	5.05	2.10
17	3.43	0.93	3.75	1.19	3.00	0.30
TS(**17**-**18**)	17.39	18.39	16.94	18.35	18.50	18.62
18	−0.42	−0.44	−0.45	−0.48	−0.41	−0.42

[a] Energies are zero-point corrected.
[b] All enthalpies and Gibbs free energies are at 298.15 K.

With regard to the key steps in our proposed catalytic cycle and considering the PPh_3 system, the oxidative addition of the iridium into the aryl C–H bond, requires a moderate activation enthalpy of 16.70 kcal mol^{-1} (Table 5, Figure 7). Furthermore, the conversion of **16** to **13** is endothermic by 3.66 kcal mol^{-1} with respect to **16**. The subsequent H/D exchange step (**13**→**17**) is calculated to be rapid, with an activation barrier of 2.25 kcal mol^{-1}. In contrast to oxidative insertion, reductive elimination is favoured enthalpically, presumably due to the decrease in steric strain within the vicinity of the metal centre. Accordingly and based on this calculated PES, we can conclude that the rate-limiting step within such H/D exchange processes appears to involve the oxidative addition or reductive elimination of the *ortho*-C–H bonds. In a complementary experimental study, we strengthened this argument by observing a primary kinetic isotope effect of approximately 3.7 (see the Supporting Information for full details). This suggests that C–H activation[21] is, indeed, rate-limiting.

Having established the relative reaction energetics in HIE reactions employing acetophenone, **6a**, attention turned to the reactivity of our catalysts with respect to different target molecules. Such studies also offered the potential to explain the selective labelling of substrates *via* a 5-mmi as opposed to a 6-mmi. Three substrates were selected for investigation: acetophenone, **6a**, 2-phenylpyridine, **6e**, and acetanilide, **6h** (Figure 8).

In view of the similar energy values calculated for complexes bearing either PPh_3 or PMe_3 as the axial ligand, the remaining theoretical studies were performed with the smaller tertiary phosphine ligand in place. As our previous explorations had supported C–H activation as being rate-determining, the effects of the alternative substrates were examined within this portion of the catalytic process (Table 6). As revealed by the activation enthalpy values the substrates labelling *via* a 5-mmi, acetophenone, **6a**, and 2-phenylpyridine, **6e**, were found to be most active. The identification of acetanilide, **6h**, as the least active substrate further supports our more general observations that compounds which are labelled *via* a 6-mmi are less reactive in our catalysed HIE reactions (*vide supra*).[5d]

Further theoretical calculations were performed to determine the binding energies of the three substrates under investigation (Table 7), since these had previously also been shown to influence labelling efficiencies.[22] The stabilisation energy, ΔH_{bind}, resulting from the complexation of the substrate to the iridium metal, forming the species akin to **16**, is calculated as

© 2014 Wiley-VCH Verlag GmbH & Co. KGaA, Weinheim

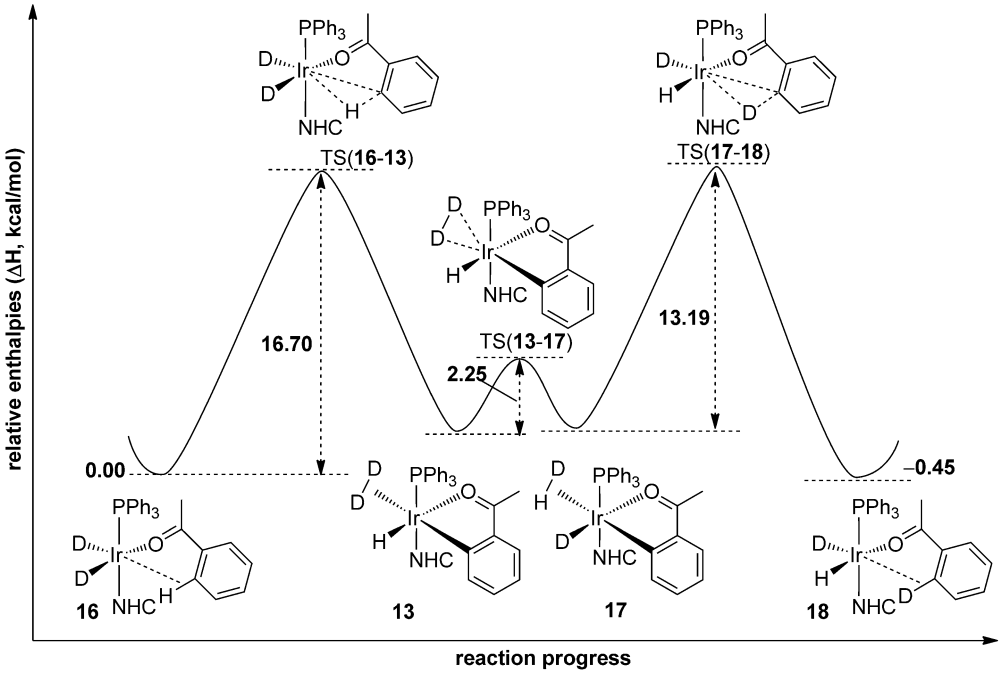

Figure 7. The reaction PES employing Ph_3P as the phosphine ligand.

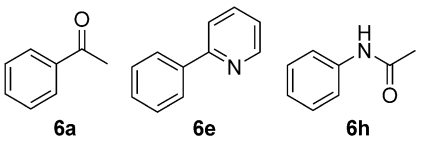

Figure 8. Substrates used in the DFT calculations.

Table 6. Enthalpy changes for the oxidative addition step with three different substrates.

Species	$\Delta H^{[a,b]}$ 6a	6e	6h
16	0.00	0.00	0.00
TS(**16-13**)	18.13	17.53	23.04
13	1.20	2.73	5.11

[a] All enthalpy changes are in kcal mol^{-1} at 298.15 K.
[b] Calculations are based on the catalyst bearing the smaller PMe_3 ligand.

Table 7. Calculated binding energies ($PR_3 = PMe_3$).

Substrate	6a	6e	6h
ΔH_{bind}[a]	−23.48	−31.42	−23.94

[a] All relative enthalpies are in kcal mol^{-1} at 298.15 K.

the difference in enthalpy between the enthalpy of the optimised complex, **16**, and the sum of the enthalpies of the optimised substrate and the optimised $[(D_2)Ir(PMe_3)(NHC)]^+$ complex. As illustrated by the values in Table 7, all complexes have a stabilising interaction enthalpy with the substrates. It should be noted that the values presented represent binding enthalpies, as opposed to free energies, and, as such, entropic effects have not been accounted for. In all cases, the entropic contribution will negatively affect the stability of the complex relative to the separated reactants.

As shown in Table 7, substrate **6e** binds most strongly to the iridium centre compared to other substrates, presumably due to the better binding ability of the more basic N atom, relative to a carbonyl O atom. In addition, substrate **6h** binds to the iridium centre with a similar strength as displayed by substrate **6a**. In both cases the coordination proceeds *via* interaction of the oxygen atom lone pair of electrons to the metal core. Hence, it can be deduced that the activation enthalpy, rather than the binding enthalpy, dictates the more effective labelling *via* a 5- over a 6-mmi.

Incorporation of Tritium

Following the success of our emerging iridium phosphine/carbene species for H/D exchange, and with an improved understanding of the catalytic mechanism, investigations were undertaken to ascertain whether these Ir species could also facilitate hydrogen–tritium exchange reactions. Since radionuclides can be detected more sensitively than stable isotopes, it is common practice within pharmaceutical laboratories to pre-

 © 2014 Wiley-VCH Verlag GmbH & Co. KGaA, Weinheim

pare both the stable isotopically-labelled molecule and the radio-labelled compound.[2c,9] Therefore, it was important to determine the activity of the developed catalysts in the labelling of substrates with tritium. Due to the more challenging hydrogen–tritium exchange process, based on the increased tritium–tritium bond strength, 5 mol% catalyst loading was required. Nonetheless, over a relatively short reaction time of only 2 h, a successful tritiation protocol was achieved (Table 8).

Tritiation *via* a 5-mmi proved relatively facile with high levels of T uptake being observed (**19b**, **19e**, **19p**). Perhaps as anticipated, hydrogen–tritium exchange through a 6-mmi was less efficient, with only 7% incorporation achieved with acetanilide, **19h**. As anticipated, only the position activated through the 5-mmi in **19j** was labelled regioselectively and with good levels of effectiveness. Of particular note was the extremely successful tritiation of the drug molecule Celecoxib, **19m**; furthermore and in contrast with the analogous deuterium experiment, only the positions *ortho* to the pyrazole directing group displayed tritium incorporation. With respect to all examples shown in Table 8, we were pleased to note that the process was remarkably clean, with no significant tritiated by-products being observed. Indeed, in previous studies we have revealed an appreciably different reaction profile, possessing an array of T-possessing by-products, when Crabtree's catalyst is employed.[9]

Table 8. Tritiation studies with catalysts **5a–c**.[a,b]

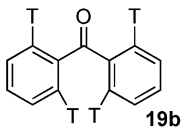

19b

5b: T_0 (3), T_1 (23), T_2 (41), T_3 (27), T_4 (7)

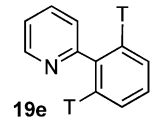

19e

5a: T_0 (15), T_1 (20), T_2 (64), T_3 (1)

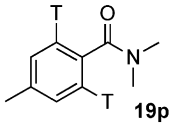

19p

5b: T_0 (64), T_1 (31), T_2 (5)

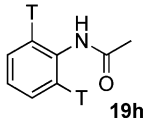

19h

5b: T_0 (93), T_1 (7)

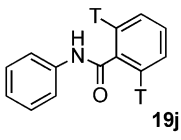

19j

5c: T_0 (15), T_1 (46), T_2 (38), T_3 (1)

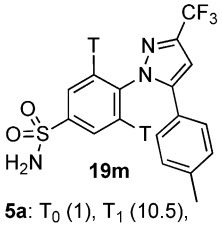

19m

5a: T_0 (1), T_1 (10.5), T_2 (87), T_3 (1.5)

[a] 5 mol% of Ir catalyst employed over 2 h.

[b] T_x (where $x = 0, 1, 2, 3, 4$) refers to the number of tritium atoms incorporated into the molecule, for example, for **19b**, T_1 (23) indicates that 23% of the sample contained one tritium atom. See the Supporting Information for further details.

Conclusions

By embedding a bulky N-heterocyclic carbene ligand in combination with different phosphine ligands, a series of highly active iridium-based catalysts has been developed for hydrogen isotope exchange. Such catalysts have been shown to produce high incorporations of deuterium and tritium adjacent to a good range of relevant functional units within a series of compounds, including pharmaceutically active agents. Additionally, combined experimental and computational studies have led to a deeper understanding of the nature of such catalyst systems and the active species generated, as well the overall reaction mechanism. These investigations have indicated that the C–H activation process is the rate-limiting step within this HIE manifold. Furthermore, the C–H activation event also constitutes the regiochemistry-determining step when both 5- and 6-metallocyclic intermediates are possible, leading to appreciable selectivities within the established exchange processes.

With regards the pivotal C–H activation, we believe that the electron-rich ligand set employed as part of the emerging catalyst systems is central to the facilitation of the requisite oxidative addition step within the catalytic cycle. Furthermore, the sterically crowded ligand sphere will, in turn, aid reductive elimination. In relation to this latter point, when sterically less demanding phosphine/NHC combinations were applied within our laboratory, the resulting complexes displayed appreciably lowered activity within HIE processes. It should also be noted that the bulky NHC and phosphine ligands used within our series of iridium complexes could provide the active catalytic species, formed within the reaction manifold, with enhanced levels of stability by preventing the existence of inactive iridium clusters[12] or driving the presence of monomeric active iridium species.[11b]

Overall, the novel catalysts developed for HIE reactions within this programme have the clear potential to replace Crabtree's catalyst as the industry standard in this area. Moreover, these complexes are stable in air and at room temperature, retaining their activity over prolonged storage periods. The experimental and computational methods employed here, aligned with the associated mechanistic and theoretical insights delivered through this study, are now being employed within our laboratory in endeavours to develop catalyst systems of further enhanced activity and more widespread substrate applicability.

© 2014 Wiley-VCH Verlag GmbH & Co. KGaA, Weinheim

Experimental Section

Computational Methods

Density functional theory (DFT) was employed to calculate the electronic structures and energies for all species involved in H/D exchange reactions. A hybrid *meta*-GGA exchange correlation functional M06[23] was used in conjunction with the 6–31G(d,p)[24] basis set for main group non-metal atoms and the Stuttgart RSC[25] effective core potential along with the associated basis set for Ir. Harmonic vibrational frequencies are calculated (with the incorporation of deuterium wherever needed) at the same level of theory to characterise respective minima (reactants, intermediates, and products with no imaginary frequency) and first order saddle points (TSs with one imaginary frequency). All calculations have been performed with the GAUSSIAN 09 quantum chemistry programme package. More detailed discussion of the computational methods, with full references, can be found in the Supporting Information.

General Procedure for the Synthesis of Complexes 5a–5e

A flame-dried and nitrogen-cooled Schlenk tube was charged with **3** and dry benzene (10 mL). The solution was treated with freshly prepared 1 M sodium ethoxide solution and stirred for 10 min. After this time, **4** was added and the mixture stirred for 5 h at room temperature. The solvent was removed under high vacuum and the residue triturated with dry ether prior to filtration through celite under N_2. After solvent exchange to dry THF (15 mL), $AgPF_6$ was added and the resultant slurry stirred for 30 min at room temperature. After filtration through celite under N_2, the solution was treated with phosphine and the resultant ruby red solution was stirred for 2 h. Purification by recrystallisation yielded the desired complex.

Standard Hydrogen Isotope Exchange Procedure

A flame-dried and nitrogen-cooled 250-mL 3-neck round-bottomed flask, equipped with two stopcock valves and a suba seal, was charged with the iridium complex (5 mol%) and dry DCM (2.5 mL), followed by the substrate (0.215 mmol). The suba seal was replaced with a greased glass stopper and the reaction vessel was cooled to −78 °C in a dry ice/acetone bath, prior to being purged twice with nitrogen. The flask was then evacuated and filled with deuterium gas *via* balloon. The flask was removed from the slurry and allowed to warm to room temperature. (***Note:*** the glass stopper must be physically restrained as the reaction mixture warms to room temperature; further standard caution should also be observed ensuring the robust nature of the glassware used and the employment of less vigorous stirring at this stage in the process). The reaction mixture was then allowed to stir vigorously at room temperature for the allotted reaction time. After this time, excess deuterium gas was removed from the system under vacuum. The reaction mixture was concentrated under reduced pressure and the catalyst complex was precipitated using diethyl ether (~ 10 mL) and removed by filtration through a plug of silica. Concentration of the filtrate under reduced pressure yielded the product/substrate mixture, which was analysed by ^{1}H NMR spectroscopy. The level of isotope incorporation into the substrate was determined by ^{1}H NMR analysis of the reaction products. As such, the residual proton signal from the site of incorporation was compared against that of a site where incorporation was not expected or occurred.

Full details of all experimental procedures, analyses, and DFT calculations (including optimised Cartesian coordinates) can be found in the Supporting Information.

Acknowledgements

We thank the University of Strathclyde (J.A.B.), AstraZeneca, R&D Mölndal (S.I. and A.R.C.), and the Carnegie Trust (M.R.) for postgraduate studentship funding. Mass spectrometry data were acquired at the EPSRC UK National Mass Spectrometry Facility at Swansea University. T.T. thanks the Glasgow Centre for Physical Organic Chemistry for funding.

References

[1] a) R. Mahajan, K. Gupta, *J. Pharm. Bioallied Sci.* **2010**, *2*, 307–313; b) J. Arrowsmith, P. Miller, *Nat. Rev. Drug Discov.* **2013**, *12*, 569–569.

[2] a) W. J. S. Lockley, *J. Label. Compd. Radiopharm.* **2007**, *50*, 779–788; b) J. Atzrodt, V. Derdau, T. Fey, J. Zimmermann, *Angew. Chem. Int. Ed.* **2007**, *46*, 7744–7765; c) E. M. Isin, C. S. Elmore, G. N. Nilsson, R. A. Thompson, L. Weidolf, *Chem. Res. Toxicol.* **2012**, *25*, 532–542; d) W. J. S. Lockley, A. McEwen, R. Cooke, *J. Label. Compd. Radiopharm.* **2012**, *55*, 235–257.

[3] For examples using platinum catalysis, see: J. L. Garnett, R. J. Hodges, *J. Am. Chem. Soc.* **1967**, *89*, 4546–4547.

[4] For examples using rhodium catalysis, see: a) M. R. Blake, J. L. Garnett, I. K. Gregor, W. Hannan, K. Hoa, M. A. Long, *J. Chem. Soc. Chem. Commun.* **1975**, 930–932; b) W. J. S. Lockley, *Tetrahedron Lett.* **1982**, *23*, 3819–3822; c) W. J. S. Lockley, *J. Label. Compd. Radiopharm.* **1984**, *21*, 45–57; d) W. J. S. Lockley, *J. Label. Compd. Radiopharm.* **1985**, *22*, 623–630; e) D. Hesk, J. R. Jones, W. J. S. Lockley, *J. Pharm. Sci.* **1991**, *80*, 887–890.

[5] For examples using iridium catalysis, see: a) R. H. Crabtree, E. M. Holt, M. Lavin, S. M. Morehouse, *Inorg. Chem.* **1985**, *24*, 1986–1992; b) R. Heys, *J. Chem. Soc. Chem. Commun.* **1992**, 680–681; c) J. R. Heys, A. Y. L. Shu, S. G. Senderoff, N. M. Phillips, *J. Label. Compd. Radiopharm.* **1993**, *33*, 431–438; d) A. Y. L. Shu, W. Chen, J. R. Heys, *J. Organomet. Chem.* **1996**, *524*, 87–93; e) L. P. Kingston, W. J. S. Lockley, A. N. Mather, E. Spink, S. P. Thompson, D. J. Wilkinson, *Tetrahedron Lett.* **2000**, *41*, 2705–2708; f) J. G. Ellames, S. J. Gibson, J. M. Herbert, W. J. Kerr, A. H. McNeill, *Tetrahedron Lett.* **2001**, *42*, 6413–6416; g) P. W. C. Cross, J. G. Ellames, J. S. Gibson, J. M. Herbert, W. J. Kerr, A. H. McNeill, T. W. Mathers, *Tetrahedron* **2003**, *59*, 3349–3358; h) B. McAuley, M. J. Hickey, L. P. Kingston, J. R. Jones, W. J. S. Lockley, A. N. Mather, E. Spink, S. P. Thompson, D. J. Wilkinson, *J. Label.*

 © 2014 Wiley-VCH Verlag GmbH & Co. KGaA, Weinheim

Compd. Radiopharm. **2003**, *46*, 1191–1204; i) J. G. Ellames, J. S. Gibson, J. M. Herbert, W. J. Kerr, A. H. McNeill, *J. Label. Compd. Radiopharm.* **2004**, *47*, 1–10; j) M. B. Skaddan, C. M. Yung, R. G. Bergman, *Org. Lett.* **2004**, *6*, 11–13; k) C. M. Yung, M. B. Skaddan, R. G. Bergman, *J. Am. Chem. Soc.* **2004**, *126*, 13033–13043; l) R. N. Garman, M. J. Hickey, L. P. Kingston, B. McAuley, J. R. Jones, W. J. S. Lockley, A. N. Mather, D. J. Wilkinson, *J. Label. Compd. Radiopharm.* **2005**, *48*, 75–84; m) J. M. Herbert, A. D. Kohler, A. H. McNeill, *J. Label. Compd. Radiopharm.* **2005**, *48*, 285–294; n) J. Krüger, B. Manmontri, G. Fels, *Eur. J. Org. Chem.* **2005**, 1402–1408; o) J. R. Heys, *J. Label. Compd. Radiopharm.* **2007**, *50*, 770–778; p) J. R. Heys, C. S. Elmore, *J. Label. Compd. Radiopharm.* **2009**, *52*, 189–200; q) R. Salter, *J. Label. Compd. Radiopharm.* **2010**, *53*, 645–657.

[6] For examples using nickel catalysis, see: J. R. Heys, *J. Label. Compd. Radiopharm.* **2010**, *53*, 716–721.

[7] a) R. H. Crabtree, H. Felkin, G. E. Morris, *J. Organomet. Chem.* **1977**, *141*, 205–215; b) R. H. Crabtree, *Acc. Chem. Res.* **1979**, *12*, 331–337.

[8] a) D. Hesk, P. R. Das, V. Evans, *J. Label. Compd. Radiopharm.* **1995**, *36*, 497–502; b) G. J. Ellames, J. S. Gibson, J. M. Herbert, A. H. McNeill, *Tetrahedron* **2001**, *57*, 9487–9497; c) S. C. Schou, *J. Label. Compd. Radiopharm.* **2009**, *52*, 376–381; d) D. Hesk, C. F. Lavey, P. McNamara, *J. Label. Compd. Radiopharm.* **2010**, *53*, 722–730; e) M. Vliegen, P. Haspeslagh, W. Verluyten, *J. Label. Compd. Radiopharm.* **2012**, *55*, 155–157.

[9] G. N. Nilsson, W. J. Kerr, *J. Label. Compd. Radiopharm.* **2010**, *53*, 662–667.

[10] H. M. Lee, T. Jiang, E. D. Stevens, S. P. Nolan, *Organometallics* **2001**, *20*, 1255–1258.

[11] a) L. D. Vásquez-Serrano, B. T. Owens, J. M. Buriak, *Chem. Commun.* **2002**, 2518–2519; b) L. D. Vázquez-Serrano, B. T. Owens, J. M. Buriak, *Inorg. Chim. Acta* **2006**, *359*, 2786–2797.

[12] Crabtree's catalyst is known to be thermally unstable and is prone to deactivation *via* the irreversible formation of inactive clusters, see a) D. F. Chodosh, R. H. Crabtree, H. Felkin, G. E. Morris, *J. Organomet. Chem.* **1978**, *161*, C67–C70; b) ref.[7]

[13] a) J. A. Brown, S. Irvine, A. R. Kennedy, W. J. Kerr, S. Andersson, G. N. Nilsson, *Chem. Commun.* **2008**, 1115–1117; b) For a recent disclosure of the use of complexes such as [(COD)Ir(IMes)Cl], a precursor to catalysts **5a–e**, in HIE processes, see A. R. Cochrane, S. Irvine, W. J. Kerr, M. Reid, S. Anderson, G. N. Nilsson, *J. Label. Compd. Radiopharm.* **2013**, *56*, 451–454. c) Catalysts **5a–c** are now available commercially from Strem Chemicals Ltd.

[14] L. S. Bennie, C. J. Fraser, S. Irvine, W. J. Kerr, S. Andersson, G. N. Nilsson, *Chem. Commun.* **2011**, *47*, 11653–11655.

[15] C. D. Forsyth, W. J. Kerr, L. C. Paterson, *Synlett* **2013**, *24*, 587–590.

[16] C. Kocher, W. A. Herrmann, *J. Organomet. Chem.* **1997**, *532*, 261–265.

[17] D. Balcells, E. Clot, O. Eisenstein, *Chem. Rev.* **2010**, *110*, 749–823.

[18] During the construction of this manuscript a study appeared divulging labelling adjacent to a *secondary* sulfonamide unit albeit at more elevated temperatures (90 °C) in a higher boiling solvent: M. Parmentier, T. Hartung, A. Pfaltz, D. Muri, *Chem. Eur. J.* **2014**, *20*, 11496–11504.

[19] a) Y.-H. Chang, C.-F. Fu, Y.-H. Liu, S.-M. Peng, J.-T. Chen, S.-T. Liu, *Dalton Trans.* **2009**, 861–867; b) O. Torres, M. Martín, E. Sola, *Organometallics* **2009**, *28*, 863–870.

[20] M. S. Sanford, M. Ulman, R. H. Grubbs, *J. Am. Chem. Soc.* **2001**, *123*, 749–750.

[21] E. M. Simmons, J. F. Hartwig, *Angew. Chem.* **2012**, *124*, 3120–3126; *Angew. Chem. Int. Ed.* **2012**, *51*, 3066–3072.

[22] A. R. Cochrane, C. Idziak, W. J. Kerr, B. Mondal, L. C. Paterson, T. Tuttle, S. Andersson, G. N. Nilsson, *Org. Biomol. Chem.* **2014**, *12*, 3598–3603.

[23] Y. Zhao, D. G. Truhlar, *Theor. Chem. Acc.* **2008**, *120*, 215–241.

[24] a) W. J. Hehre, R. Ditchfield, J. A. Pople, *J. Chem. Phys.* **1972**, *56*, 2257–2261; b) M. M. Francl, W. J. Petro, W. J. Hehre, J. S. Binkley, M. S. Gordon, D. J. DeFrees, J. A. Pople, *J. Chem. Phys.* **1982**, *77*, 3654–3665.

[25] D. Andrae, U. Häußermann, M. Dolg, H. Stoll, H. Preuß, *Theor. Chim. Acta* **1990**, *77*, 123–141.

 © 2014 Wiley-VCH Verlag GmbH & Co. KGaA, Weinheim